Journal of Electromagnetic Waves and Applications

ISSN: 0920-5071 (Print) 1569-3937 (Online) Journal homepage: http://www.tandfonline.com/loi/tewa20

Simulation and validation of radio frequency heating with conveyor movement

L. Chen, Z. Huang, K. Wang, W. Li & S. Wang

To cite this article: L. Chen, Z. Huang, K. Wang, W. Li & S. Wang (2016) Simulation and validation of radio frequency heating with conveyor movement, Journal of Electromagnetic Waves and Applications, 30:4, 473-491, DOI: 10.1080/09205071.2015.1121841

To link to this article: http://dx.doi.org/10.1080/09205071.2015.1121841

JOURNAL OF ELECTROMAGNETIC WAVES AND APPLICATIONS, 2016
VOL. 30, NO. 4, 473–491
http://dx.doi.org/10.1080/09205071.2015.1121841

Taylor & Francis
Taylor & Francis Group

Simulation and validation of radio frequency heating with conveyor movement

L. Chen[a], Z. Huang[a], K. Wang[a], W. Li[a] and S. Wang[a,b]

[a]College of Mechanical and Electronic Engineering, Northwest A&F University, Yangling, Shaanxi 712100, China; [b]Department of Biological Systems Engineering, Washington State University, Pullman, WA 99164-6120, USA

ABSTRACT

Computer simulation is widely used as a valuable tool to systematically study radio frequency (RF) heating with time-saving and effective cost. A computer simulation model using finite element-based commercial software, COMSOL, was developed to simulate temperature distributions in wheat samples packed in a rectangular plastic container and treated in a 6 kW, 27.12 MHz RF system under stationary and moving conditions. Both simulated and experimental results showed similar heating patterns in RF-treated wheat samples, in which corners and edges were more heated and the temperatures were higher in the lower sections of the container. The simulation results demonstrated that the RF heating uniformity could be improved by conveyor movement and selecting the top electrode area similar to the sample size. The validated model can be further applied to optimize parameters of conveyor movement and top electrode configuration to improve RF heating uniformity.

ARTICLE HISTORY
Received 11 November 2014
Accepted 16 November 2015

KEYWORDS
RF heating; wheat; computer simulation; movement; top electrode; heating uniformity

1. Introduction

Radio frequency (RF) heating involves utilizing electromagnetic energy at a frequency range of 3 kHz to 300 MHz. Because of its rapid and volumetric heating, the RF treatment has been studied for pasteurization,[1–3] disinfestations [4–7] in postharvest agricultural products, and tissue heating.[8,9] The major obstacle for implementing RF technology in industrial applications is the non-uniform heating.[10,11] The hot and cold spots may cause quality loss and microbial or insect pest survivals in RF-treated products.[1,12–14] Many engineering approaches have been used in research laboratories to improve the RF heating uniformity, such as hot air surface heating, movement, and mixing.[10,15–17] Since in commercial systems, materials often move in a continuous mode to achieve desired capacities, it is important to clearly determine the effects of conveyor movement on temperature distributions in RF-treated products for developing industrial postharvest disinfestations.

Movement and rotation of samples have been reported to improve heating uniformity in RF and microwave systems. Uniform heating has been achieved by the implementation

CONTACT S. Wang shaojinwang@nwsuaf.edu.cn

of a two-stage rotation of vegetable cups during microwave processing.[18] Sample movement optimization is applied for achieving uniform temperature distributions within microwave-heating applicators.[19] Acidified vegetable packages are placed on a conveyor belt through a 3.5 kW, 915 MHz microwave cavity, resulting in good retention of color and texture after achieving required pasteurization levels.[20] Back and forth movements on the conveyor belt are widely used in RF systems to improve heating uniformity in almonds,[16] legumes,[21] coffee beans,[17] and lentils.[10] With rotation and movement of apples, oranges, and persimmons using a fruit mover, RF heating uniformity has been significantly improved. [22–24] Although many experiments prove that movements can improve heating uniformity of products, there is no computer simulation model to systematically study the effect of conveyor movement on RF heating uniformity.

To understand the complex mechanisms on the heating uniformity of food products subjected to RF treatments, mathematical modeling and computer simulation are commonly used as valuable tools with time-saving and effective cost. A circuit model of a RF industrial system is developed [25], and electric fields inside RF applicators are determined by solving both wave and Laplace equations using finite element methods.[26] Chan et al. [27] presented an effective approach to modeling industrial RF heating systems using the wave equation applied in three dimensions. To study the RF heating uniformity, several simulation models have been developed for different food materials, such as radish seeds,[28] meat batters,[29] mashed potatoes,[30] wheat flour,[13] and raisins.[14] Although the influence of intermittent stirrings on RF heating uniformity is determined, the mathematical model is developed based on normal sample temperature distributions without detailed simulation of heating patterns influenced by stirring.[15] Simulations of movement in both RF and microwave heating include linear motions and rotational movements. Birla et al. [31] simulated the rotation of fruit immersed in water for RF heating in pilot scale systems to mimic industrial applications. Most of rotational simulations are for microwave heating in domestic ovens.[32–34] Linear motions in pilot scale systems to mimic industrial microwave systems have been simulated by Chen et al. [35] using FDTD method, and more recently by Resurreccion et al. [36] in a 915 MHz single-mode microwave-assisted thermal sterilization system consisting four microwave heating cavities. But few have been used in computer simulations to study RF heating uniformity in both linear and rotation motions.

The objectives of this study were to (1) develop a computer simulation model for wheat samples at a 6 kW, 27.12 MHz RF system using commercial finite element software COMSOL, (2) validate the computer simulation model by comparing with the experimental temperature profiles of wheat at three layers after RF heating under stationary and conveyor movement conditions, and (3) apply the validated model to evaluate the effects of conveyor movement, three different top electrode lengths, and turning a container by 90° under moving conditions on RF heating patterns based on the uniformity index.

2. Materials and methods

2.1. Materials and sample preparation

The wheat (*Triticum aestivum*) sample was obtained from a local farmer in Yangling, Shaanxi, China, and stored at 25 °C in a thermostatic and the relative humidity (65% RH)-controlled chamber (BSC-150, Shanghai BoXun Industrial & Commerce Co., Ltd, Shanghai,

China) prior to RF treatments. The initial moisture content of wheat was 8.7% on wet basis (w.b.). The wheat samples were placed in a rectangular container (inner dimension 300 mm × 220 mm × 60 mm) for RF treatments. The bottom and side walls of the container were made of thin polypropylene mesh (mesh diameter of 6.5 mm) with 3 mm thickness. To prevent wheat leakage from the container, the internal surface of the container was covered by a thin layer of plastic film with mesh opening of 1 mm.

2.2. Development of computer model

2.2.1. Physical model

A 6 kW, 27.12 MHz parallel plate RF heating system with a free-running oscillator (COMBI 6-S, Strayfield International Limited, Wokingham, UK) was used in this study. The RF system consisted of metallic enclosure, generator, and RF applicator with top and bottom electrodes (Figure 1). The bottom electrode was integrated into metallic enclosure. The electrode gap can be regulated by changing the position of the top electrode. The sample was placed on the conveyor belt above the bottom electrode and sandwiched between top and bottom electrodes. The dielectric material was heated up because of thermal energy converted from the electromagnetic energy.

2.2.2. Governing equations

2.2.2.1. Electric current. Since the wavelength in the 27.12 MHz RF system is often much larger than the RF cavity size (1.29 m × 1.09 m × 0.74 m), a quasi-static assumption was used to simplify Maxwell's equations to Laplace ones [37]:

$$-\nabla \cdot \left(\left(\sigma + j2\pi f\varepsilon_0\varepsilon'\right)\nabla V\right) = 0 \tag{1}$$

where σ is the electrical conductivity of the heated sample (S m^{-1}), $j = \sqrt{-1}$, ε_0 is the permittivity of free space (8.86×10^{-12} F m^{-1}), ε' is the dielectric constant of food material, and V is the voltage between the two electrodes (V). The voltage V could be related to the electric field intensity $|E_m|$ (V/m) in the food sample with $|E_m| = -\nabla V$.

2.2.2.2. Heat transfer. The heat conduction was taken into account within the food material, convection at the sample's surface, and heat generation in the food due to RF energy. The governing equation of heat transfer inside the sample is described as:

$$\frac{\partial T}{\partial t} = \nabla\alpha\nabla T + \frac{Q}{\rho C_p} \tag{2}$$

where $\partial T/\partial t$ is the heating rate in food samples (°C s^{-1}), α is the thermal diffusivity (m^2 s^{-1}), ρ and C_p are the density (kg m^{-3}) and specific heat (J kg^{-1} K^{-1}), respectively. Q is the RF power conversion to thermal energy (W m^{-3}) within the food sample under an electric field intensity ($\vec{E}_m$, V m^{-1}) and described as [38]:

$$Q = 2\pi f\varepsilon_0\varepsilon''\left|\vec{E}_m\right|^2 \tag{3}$$

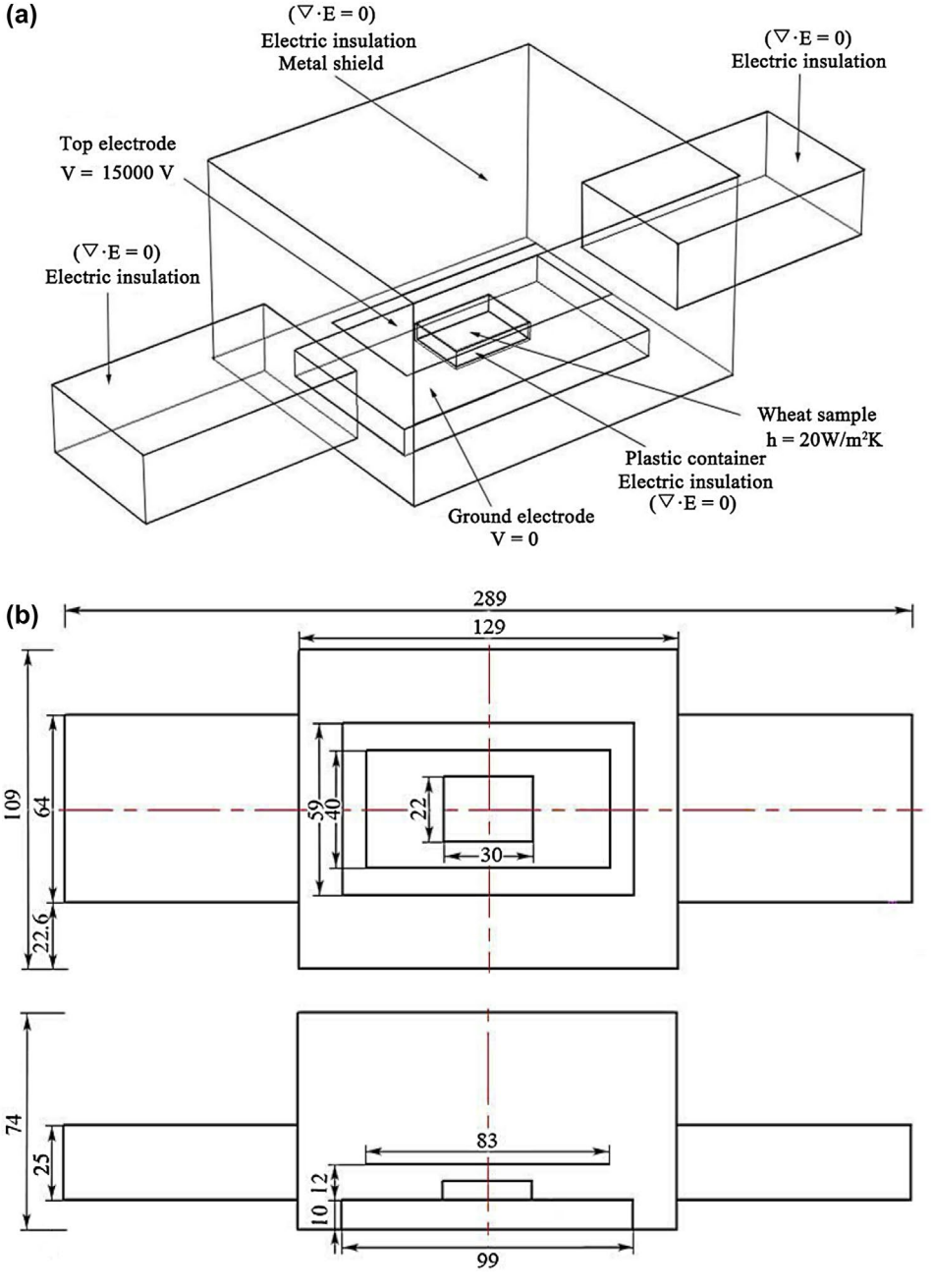

Figure 1. 3-D Scheme (a) and dimensions (b) of the RF system and food load (wheat sample) used in simulation (all dimensions are in cm) (adapted from Huang et al. [40]).

where f is the frequency of RF unit (Hz) and $|\vec{E}_m|$ is the magnitude of electric field intensity (V m^{-1}) in the food sample and described as [39]:

$$|\vec{E_m}| = \frac{V}{\sqrt{\left(\varepsilon' d_0 + d_m\right)^2 + \left(\varepsilon'' d_0\right)^2}} \tag{4}$$

where ε'' is the loss factor of the food sample, d_0 and d_m are the air gap (m) and the height (m) of the material, respectively.

2.2.3. Geometrical, thermal, and electrical boundary conditions

Figure 1(a) and (b) show the geometrical, thermal, and electrical boundary conditions of the RF system used in the simulation. The initial temperature was set at 25 °C. Except for the top uncovered surface exposed to the ambient air, the side and bottom of the sample were surrounded by the rectangular plastic container (Figure 1(a)). The top exposed surface of the sample was assigned with convective heat transfer ($h = 20\ \mathrm{W\ m^{-2}\ K^{-1}}$) for natural convection of ambient air.[14,40,41] Thermal insulation ($-\nabla T = 0$) was assigned to the metal enclosure of RF system. The electrical potential of top electrode was assumed to be uniformly distributed because its size (83 cm × 40 cm) was only 30% of the RF wavelength at 27.12 MHz (11 m), which was reported by Barber [42]. The bottom electrode was set as ground ($V = 0$ V). Since it is difficult to precisely measure the high voltage during the RF operation without disturbing the electric field,[43] the voltage on the top electrode was assumed to be constant and estimated using the equation proposed by Birla et al. [31] based on the measured heating rate. With the preliminary tests, the voltage of top electrode was estimated to be 15,000 V for further simulation runs. The same method has been used to estimate the top electrode voltage of similar RF systems.[13,14,31]

2.2.4. Model development under conveyor movement

2.2.4.1. Model assumptions. To simulate the temperature distributions in the wheat sample after conveyor movement, the following assumptions were considered:

(1) When the sample container was fully covered (P2–P4) by the top electrode during the moving process (Figure 2), the voltage (V_{\text{m}}) and electric field distributions were assumed to be uniform. The non-uniform electric field distribution in sample at different positions was neglected since the final temperatures were taken into account after the sample passed through the symmetric electric field conditions.
(2) The changing trends of RF heating power (Q) were symmetric, when the sample container moved into (P1–P2) and out (P4–P5) of the RF system (Figure 2).
(3) The initial temperature was considered as homogeneous and isotropic throughout the wheat samples.
(4) The mass and momentum transfers of moisture were not considered due to short heating for disinfestations.

2.2.4.2. Model descriptions. In the continuous RF heating process with the conveyor belt, the sample container was moved from right side (P1) to left side (P5) (Figure 2). At different positions in the RF system, the RF heating power Q ($\mathrm{W\ m^{-3}}$) varied from position 1 (P1) to position 2 (P2) and from position 4 (P4) to position 5 (P5) according to the changed power with positions in the RF-treated walnuts [44] and lentils.[10] Specifically, before the container entered or after exited the RF cavity, the voltage (V_m) or the RF power (Q) at P1 and P5 was

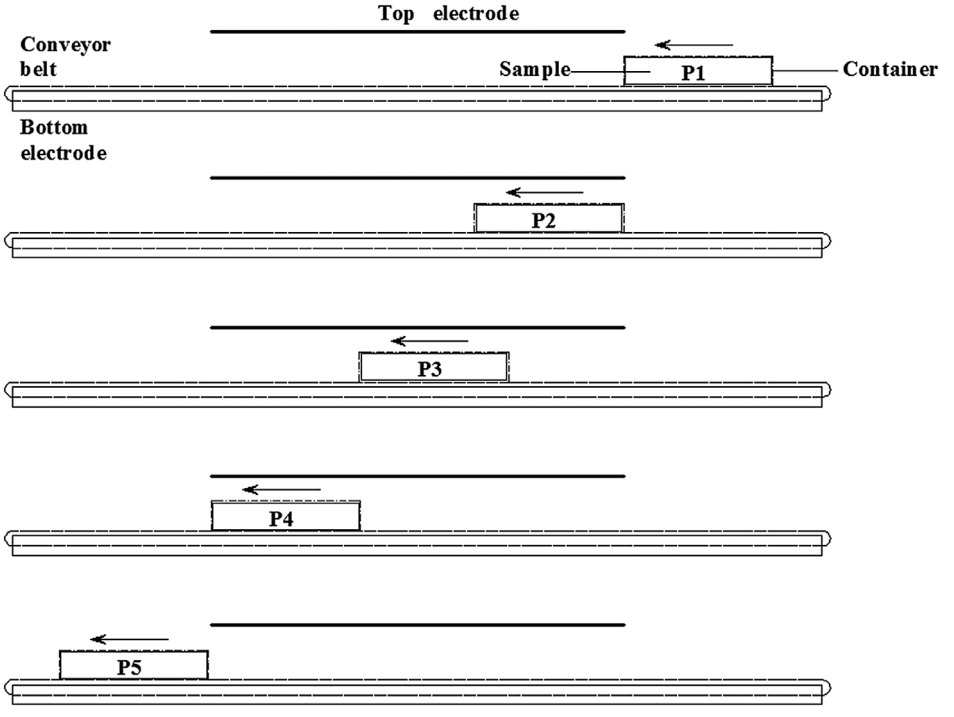

Figure 2. Five representative horizontal positions (P1–P5) during the continuous process of conveyor movement in RF systems.

at the minimum value. The RF power increased to maximum value as the container moved into the system (P2) within the transition time t_0 and eventually stabilized after the container reached the far edge of the top electrode (P4). This transition time t_0 from P1 to P2 was 76 s at the conveyor speed (v) of 14.23 m h^{-1} and calculated by Equations (5) and (6):

$$v = \frac{a * 3600}{t_1} \tag{5}$$

$$t_0 = \frac{b * 3600}{v} \tag{6}$$

where a is the length of top electrode ($a = 0.83$ m), t_1 is the heating time in the stationary experiment ($t_1 = 210$ s), and b is the length of container ($b = 0.3$ m). The RF power changing trend during this whole process could be assumed as a function of time (t, s) and positions using a power ratio, $pw(t)$, during the whole moving process (287 s) at the conveyor speed of 14.23 m h^{-1} (Figure 3). The Equation (3) becomes:

$$Q = 2\pi f \varepsilon_0 \varepsilon'' \left|\vec{E}_m\right|^2 pw(t) \tag{7}$$

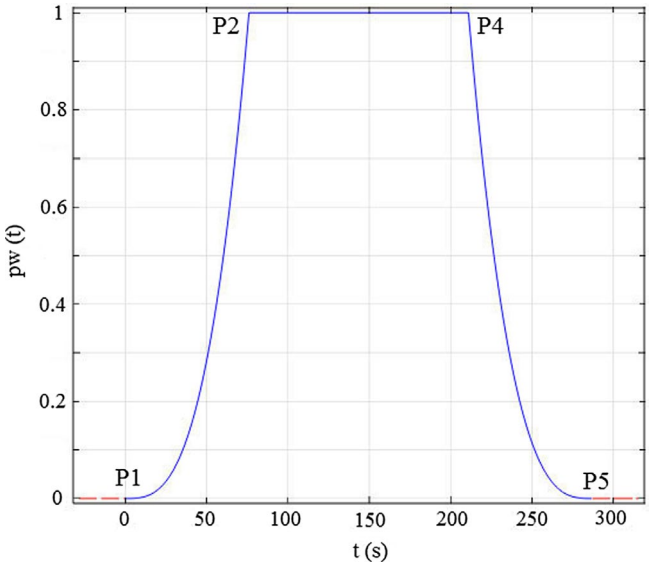

Figure 3. Assumed RF heating power ratio as a function of heating time and positions (Q, W m^{-3}) during the whole moving process (287 s) at the conveyor speed of 14.23 m h^{-1}.

The power ratio, *pw(t)*, was determined under three periods of time based on equivalent power absorption over the whole volume of the sample to stationary conditions as follows:

$$Q_{\text{movement}} * \frac{\text{V}^* \Delta \text{t}}{t_0} = Q_{\text{station}} * \text{V} * \text{pw}(t) \tag{8}$$

By inputting the RF power for movement and stationary conditions according to Equation (3), the power ratio was derived from Equation (8) with successive Δt during the whole moving time as follows:

$$pw(t) = \frac{\text{t}^3}{t_0^3} \tag{9}$$

If the transition time t_0 from P1 to P2 was 76 s, the power ratio at three durations became:

$$pw(t) = \begin{cases} \frac{t^3}{76^3} & t \in (0, 76) \\ 1 & t \in (76, 211) \\ \frac{(287-t)^3}{76^3} & t \in (211, 287) \end{cases} \tag{10}$$

Equation (7) was the heating power of sample with conveyor movement in the model, and the temperature distributions after movement were obtained using computation for 287s RF heating.

2.2.5. Solution methodology

A finite element method-based commercial software, COMSOL Multiphysics (V4.3a COMSOL Multiphysics, CnTech Co., Ltd, Wuhan, China), was used to solve the coupled electromagnetic and

heat transfer equations simultaneously. Inbuilt modules electric current (ec) and heat transfer in solid (ht) with transient analysis were selected to solve Equations (1)–(7). The software was run on Hewlett-Packard workstation with a Core (TM) i5-2400, 3.10 GHz Intel Core Processor, and 8 GB RAM operating with Windows 7 64-bit operating system. Figure 4 illustrates the steps taken in the simulation. Extremely fine mesh was created near the sharp edges and corners of the wheat sample and container to improve the accuracy of the results. The mesh size was determined based on the convergence study when the temperature difference between successive calculations was less than 0.1%. The final mesh system that consisted of 318,984 domain elements (tetrahedral), 39,298 boundary elements (triangular), 1414 edge elements (linear), and 52 vertex elements was used in subsequent simulation runs. Initial and maximum time steps were set as 0.001 and 1 s. Each computation took about 22 min.

2.2.6. Model parameters

Knowledge on dielectric, thermal, and physical properties of the sample material and surrounding medium is essential in modeling the RF heating process. Table 1 lists these values of wheat, polypropylene, aluminum, and air for computer simulation. Dielectric and thermal properties of bulk wheat samples are dependent on temperature and moisture content and obtained by Li et al. [47] and Shrestha and Baik [7]. The average values of bulk wheat properties over the tested temperature and moisture range can be found in Table 1.

2.3. Model validation

2.3.1. Stationary experiment

About 3.39 kg wheat with bulk density of 860 kg m^{-3} was put into the rectangular container in experiments as used in simulation and placed at the center of the ground electrode. Two very thin polypropylene films were used to separate the container into three layers with each filled with wheat of 1.13 kg (Figure 5), which are convenient to map the surface temperature distributions in three layers (top, middle, and bottom) using thermal imaging camera after RF heating. Prior to the RF treatment, the wheat was equilibrated at room temperature at 25 °C for 12 h. The wheat sample was subjected to stationary RF heating for 3.5 min with 120 mm electrode gap until the central sample temperature reached 45 °C, which was monitored and recorded by a fiber optic sensor system (HQ-FTS-D120, Xi'an HeQi Opo-electronic Technology Co., LTD, Shaanxi, China) with an accuracy of ±1 °C. After the RF system was turned off, the container was immediately moved out for the surface temperature mapping of all three layers of wheat starting from top to bottom layer by an infrared camera (DM63-S, DaLi Science and Technology Co., LTD, Zhejiang China) with an

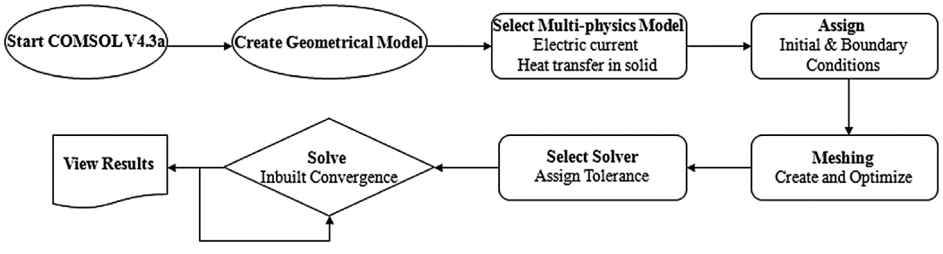

Figure 4. Flowchart of modeling steps using COMSOL Multiphysics.

Table 1. Electrical and thermo-physical properties of materials used in computer simulation.

Material properties	Wheat	Aluminum[a]	Air[a]	Polypropylene[a]
Heat capacity C_p(J kg^{-1} K^{-1})	2670[d]	900	1200	1800
Density ρ(kg m^{-3})	860	2700	1.2	900
Thermal conductivity k (W m^{-1} K^{-1})	0.15[c]	160	0.025	0.2
Dielectric constant (ε')	4.3[d]	1	1	2.0[b]
Loss factor (ε'')	0.11[d]	0	0	0.0023[b]

[a]COMSOL material library, V4.3a.[45]
[b]von Hippel. [46]
[c]Li et al. [47]
[d]Shrestha and Baik [7].

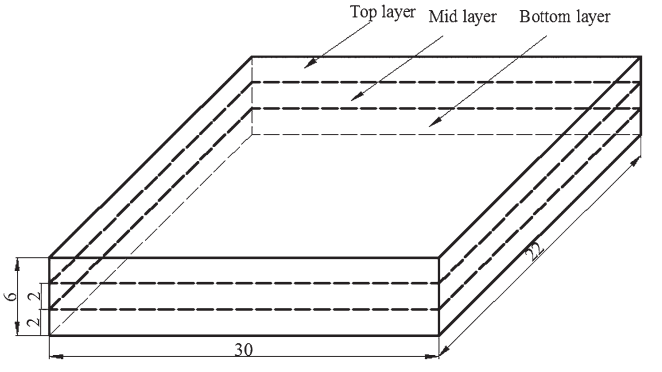

Figure 5. Rectangular plastic container divided into three layers for surface temperature measurements (all dimensions are in cm).

accuracy of ±2 °C. Details on the measurement procedure can be found in Wang et al. [44]. All the three thermal imaging recordings were completed in 30 s. The experiments were replicated two times. Experimental and simulated stationary temperature profiles of wheat were compared in the container center and at three layers.

2.3.2. Moving experiment

The same wheat sample was put on the conveyor belt at P1 (Figure 2), and conveyor speed was set at 14.3 m h^{-1} with a fixed electrode gap of 120 mm for 287 s RF heating. After RF heating with conveyor movement, the sample was moved out from P5 (Figure 2) for the surface temperature mapping of three layers. The thermal imaging procedure was the same as stationary experiment described above. Experimental and simulated moving temperature profiles of wheat samples were compared at three layers.

2.4. Model applications

After the validation of the model, the uniformity index (λ) was used to evaluate the effects of conveyor movement, three different lengths of the top electrode, and turning the container from Position A to Position B by 90° (Figure 6) under moving conditions on RF heating patterns using simulation. The uniformity index (λ) value has been used to evaluate the temperature distribution of samples subjected to RF heating,[13,14] which is defined as the

ratio of standard deviation to average temperature rise during heating, using the following equation [15] :

$$\lambda = \frac{\Delta\sigma}{\Delta\mu} \tag{11}$$

where $\Delta\sigma$ is the rise in standard deviation of product temperature and $\Delta\mu$ is the rise in mean product temperature over treatment time. In RF treatments, the smaller index represents better heating uniformity.

Conveyor belt movement with three top electrode lengths (a_1 = 0.5 m, a_2 = 0.83 m, and a_3 = 1 m) was simulated to predict their influences on heating uniformity in RF systems. Based on Equations (5) and (6), three lengths of the top electrode corresponded to conveyor belt speeds of v_1 = 8.57 m h^{-1}, v_2 = 14.23 m h^{-1}, and v_3 = 17.14 m h^{-1}, and the transition times of t_{01} = 126 s, t_{02} = 76 s, and t_{03} = 63 s, respectively. However, the transition times of placing the container at Position B were t_{04} = 93 s, t_{05} = 56 s, and t_{06} = 46 s, respectively.

3. Results and discussion

3.1. Simulated temperature distributions for wheat sample

The simulated temperature profiles of RF-treated wheat in three horizontal (20, 40, and 60 mm), three vertical (50, 150, and 250 mm) layers, and whole samples are shown in Figure 7(a)–(c) after 3.5 min stationary RF heating at a fixed electrode gap of 120 mm. In the horizontal layers, the sample temperatures were higher in the middle and the bottom layers (44–70 °C and 45–69 °C), but lowest in the top layer (43–68 °C). The average temperature of the bottom layer was slightly higher than that of the middle layer, which might be caused by more RF energy absorbed in the bottom layer due to concentrated electric field in lower sections of wheat samples. Similar results were observed by Birla et al. [31] and Marra et al. [29]. The lowest temperature of the top layer could be resulted from the heat loss and the evaporative cooling effect on the outer surface of the wheat. In the vertical layers, the sample temperature increased from the middle section to the outer section, whereas was lower at the interface of side walls of the polypropylene container. Hot spots were observed at the edges and corners of the top, middle, and bottom layers (Figure 7(a)), which could

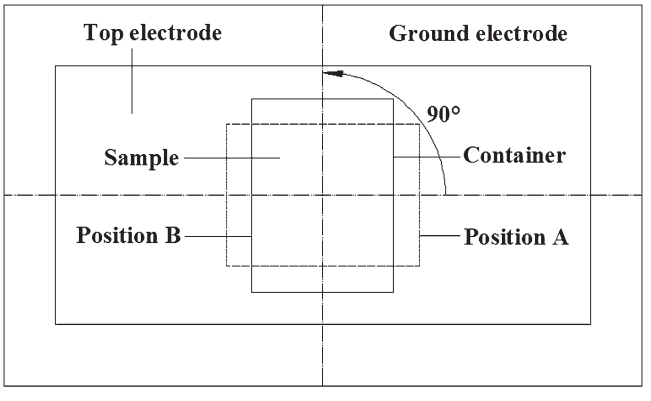

Figure 6. The container with wheat samples turned 90° from Position A to Position B used in the simulation.

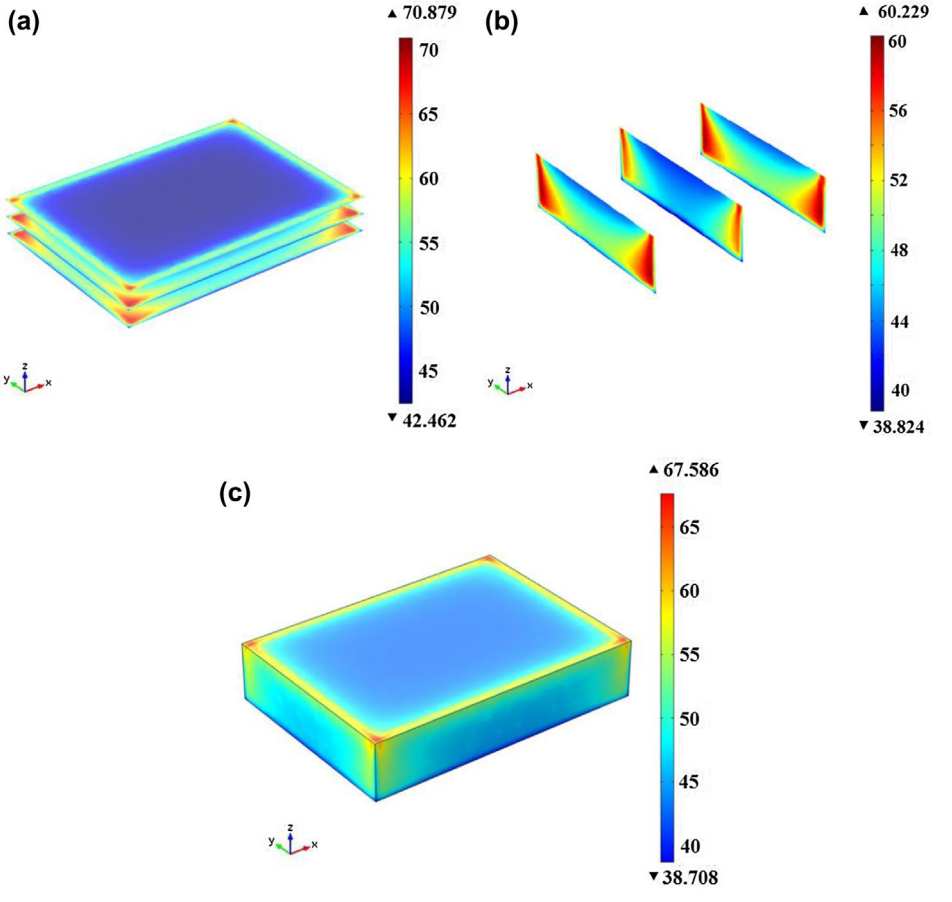

Figure 7. Simulated temperature profiles (°C) of wheat samples (300 mm × 220 mm × 60 mm) at (a) three horizontal layers (20, 40, and 60 mm), (b) three vertical layers (50, 150, and 250 mm), and (c) whole samples after 3.5 min stationary RF heating with an electrode gap of 120 mm and initial temperature of 25 °C.

be attributed to the deflected electric field at those sections. Since the RF power density at any sample location is proportional to the square of electric field, higher temperature values were observed at these parts [13]. Similar heating patterns were reported for model fruit immersed in water,[31] dried fruit,[14] fresh fruit,[22] and walnuts.[44,48]

3.2. Model validation under stationary conditions

Figure 8(a) presents the experimental surface temperatures of the wheat sample in three horizontal layers: top, middle, and bottom after 3.5 min stationary RF treatment at a fixed gap of 12 cm and an initial temperature of 25 °C. In general, the experimental heating patterns matched well with the simulated results (Figure 8(b)). Both the corners and edges of all three layers showed higher temperatures, and lower temperatures appeared in the central sections. The maximum temperature differences were found to be about 1, 3, and 5 °C at the corners and edges of top, middle, and bottom layers, respectively, when comparing between the experimental and simulated data. The experimental time–temperature history

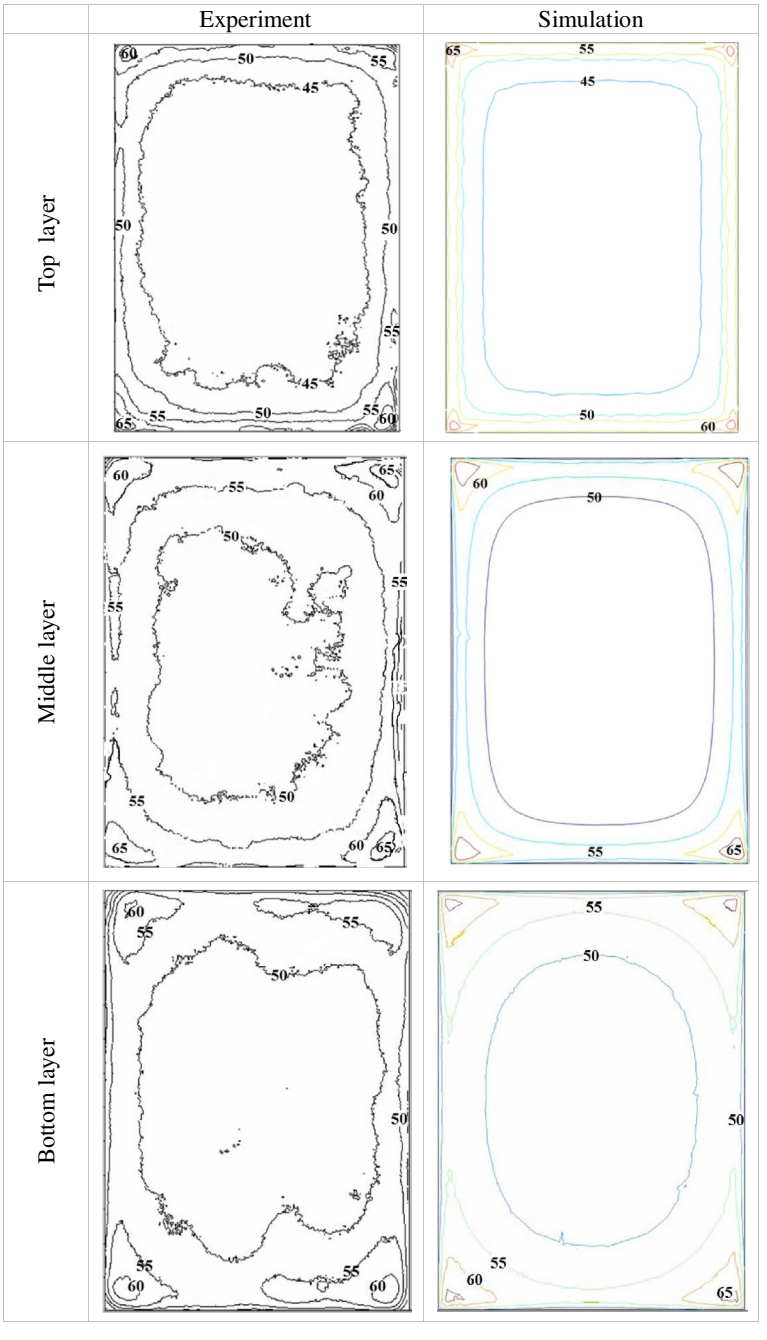

Figure 8. Experimental and simulated temperature distributions (°C) of wheat samples at top, middle, and bottom layers (20, 40, and 60 mm from the bottom of sample) in a polypropylene container (300 mm × 220 mm × 60 mm) on the center of the ground electrode, after 3.5 min stationary RF heating with an initial temperature of 25 °C and a fixed electrode gap of 120 mm.

of the central point of middle layer also showed good agreements with the simulated one (Figure 9). A comparison between the experimental and simulated average and standard deviation temperatures (°C) of wheat samples in three horizontal layers was shown in Table 2 after 3.5 min stationary RF heating at a fixed gap of 120 mm. Less than 1 °C was obtained between experimental and simulated average temperatures in all three layers, suggesting an acceptable model precision. But the simulated standard deviations were comparatively higher than those determined by experiments, which may be due to the finer mesh of corners and edges than those in central parts of wheat samples in the model. The temperature differences between experiment and simulation might be caused by the simplification of the RF units or ignored water and heat loss in the possible evaporation in the wheat sample.

3.3. Model validation under moving conditions

Figure 10 presents the experimental and simulated surface temperature distributions of the wheat sample in three horizontal layers after 287 s RF treatments at a fixed gap of 12 cm with conveyor speed at 14.23 m h^{-1}. In general, the experimental temperature contour in three layers showed a good agreement with the simulated results. However, in corners and edges of the top, middle, and bottom layers, the maximum temperature differences were about 1, 3, and 3 °C, respectively. Table 3 compared the simulated and experimental average and standard deviation temperatures of wheat samples in all three horizontal layers after 287 s moving RF heating. Less than 1 °C was obtained between experimental and simulated average temperatures in all three layers after conveyor movement. The values of simulated standard deviations were also higher than the experimental ones.

3.4. Model applications

Table 4 summarizes the values of uniformity index of three layers and the whole wheat samples in the plastic container at stationary and moving conditions both from experiment and computer simulation. The uniformity index showed the same decreasing trend from

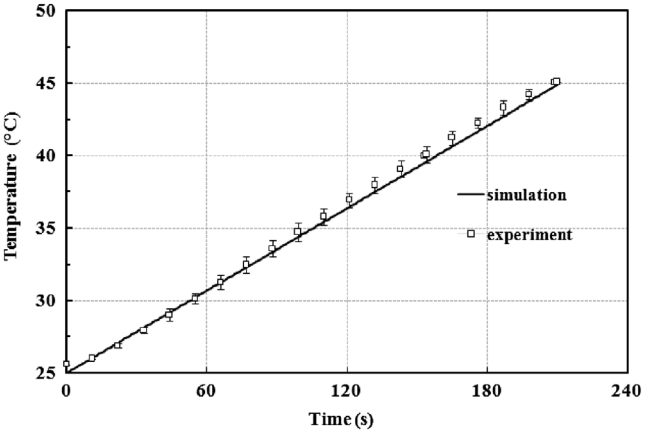

Figure 9. Experimental and simulated temperature–time histories of wheat samples at the center of second mid layer (40 mm) from the bottom of the sample (300 mm × 220 mm × 60 mm), placed in a polypropylene container on the center of the bottom electrode during 3.5 min stationary RF heating with an electrode gap of 120 mm.

Table 2. Comparison between experimental and simulated average and standard deviation temperatures (°C) of wheat samples at three horizontal layers after 3.5 min stationary RF heating at a fixed gap of 120 mm and initial temperature of 25 °C.

Layer	Experiment (°C)	Simulation (°C)
Top	49.1 ± 4.63	49.5 ± 5.46
Middle	51.5 ± 4.35	52.0 ± 5.21
Bottom	51.8 ± 3.47	52.1 ± 4.47

stationary to movement conditions and from top to bottom layers both in experiment and simulation. It is clear that the movement of conveyor belt did improve the RF heating uniformity of wheat samples, especially in the middle layer ($p < 0.05$), but it was not improved significantly ($p > 0.05$) through the whole sample. To get a better heating uniformity, we should combine conveyor movement with adding forced hot air and mixing, which were suggested in the literature.[10,16,17,21,22]

Table 5 presents uniformity index values of wheat samples at Position A (Figure 6) at three speeds of conveyor belt (v_1 = 8.57 m h^{-1}, v_2 = 14.23 m h^{-1}, and v_3 = 17.14 m h^{-1}) and total treating time (t_1 = 336 s, t_2 = 287 s, and t_3 = 273 s) corresponding to three top electrode lengths (a_1 = 0.5 m, a_2 = 0.83 m, and a_3 = 1 m). During RF heating with movement at a fixed gap of 120 mm, lower speeds of movement had a better heating uniformity ($\lambda_1 < \lambda_2 < \lambda_3$). That may be caused by heat transfer to reduce the temperature difference between cold and hot spots in wheat samples during longer heating time with lower speeds. In addition, the heating uniformity was improved by the top electrode length of 0.5 m, whose length was similar to the sample size (the length of container) since the maximum temperature of the middle layer was reduced from 67 to 60 °C. The same results have also been observed for wheat flour [13] and soybean [40] subjected to RF treatment.

Table 5 also presents uniformity index values of wheat samples after turning the container by 90° at Position B (Figure 6) with three speeds of conveyor belt (v_1 = 8.57 m h^{-1}, v_2 = 14.23 m h^{-1}, and v_3 = 17.14 m h^{-1}) and total heating time (t_1 = 302 s, t_2 = 266 s, and t_3 = 256 s) corresponding to the three top electrode lengths. The same trend was found as the wheat samples at Position A. For example, lower speeds of conveyor movement had better uniformity. In addition, when comparing the uniformity index between these two different positions, we found that uniformity index values were reduced after turning the container by 90° (Position B). That may be caused by the improved electric fields in samples since the length of the container (0.3 m) was closer to the width of the top electrode (0.4 m) after turning the container.

3.5. Limitation of the model

The simulation model developed in this study was able to predict the final-state temperature profiles based on equivalent power absorption over the whole volume of the sample, using average values of thermal and dielectric properties of wheat samples over the given temperature range. The validated model was further used to predict the influences of conveyor movement, three different top electrode lengths, and turning the container by 90° under moving conditions on heating uniformity. In the current model, however, the assumed constant voltage and uniform electric field distributions over the entire top electrode (P2–P4) may not be true due to the observed different sample temperatures located in different

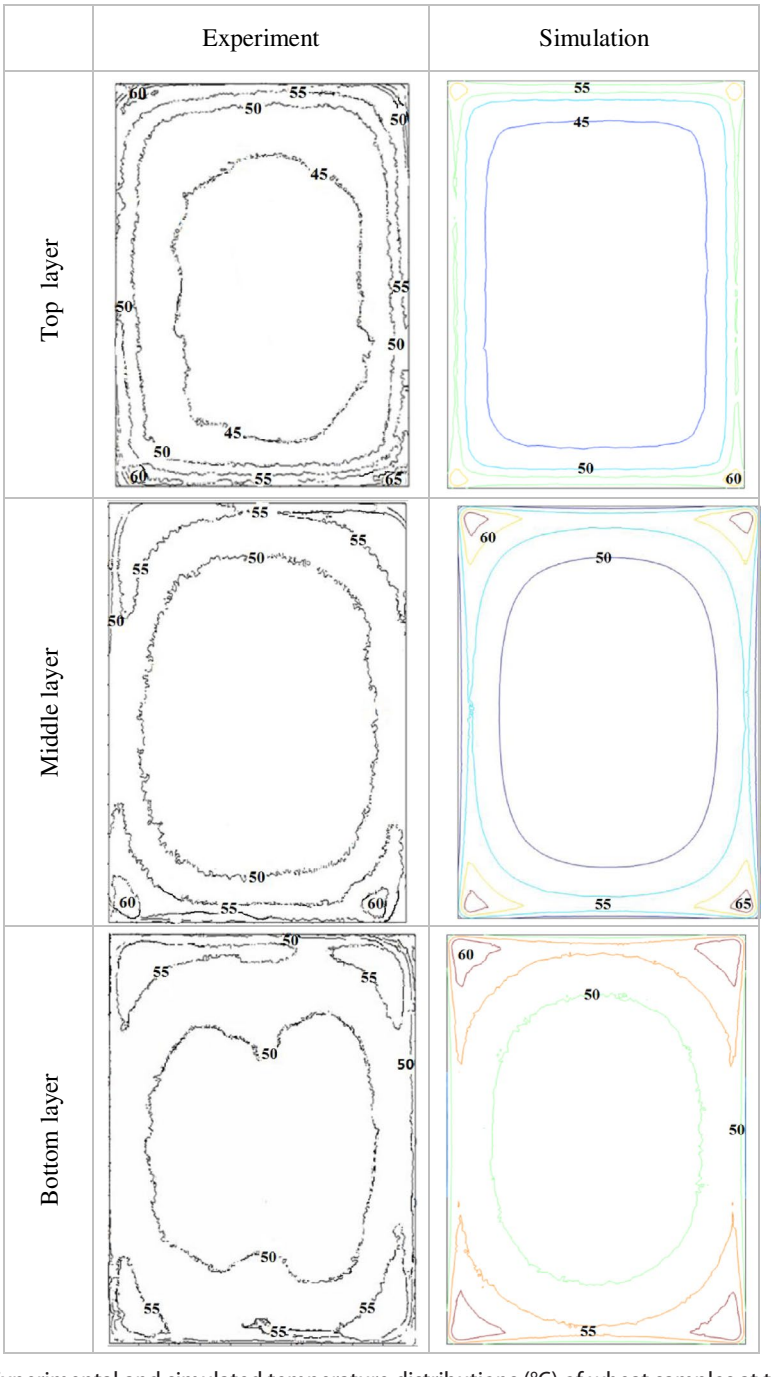

Figure 10. Experimental and simulated temperature distributions (°C) of wheat samples at top, middle, and bottom layers (20, 40, and 60 mm from the bottom of samples) in a polypropylene container (300 mm × 220 mm × 60 mm) with conveyor movement at the speed of 14.23 m h^{-1}, after 287 s RF heating with an initial temperature of 25 °C and a fixed electrode gap of 120 mm.

Table 3. Comparison between experimental and simulated average and standard deviation temperatures (°C) of wheat samples at three horizontal layers with conveyor movement at the speed of 14.23 m h^{-1} after 287 s RF heating with an initial temperature of 25 °C and a fixed electrode gap of 120 mm.

Layer	Experiment (°C)	Simulation (°C)
Top	49.1 ± 4.54	47.8 ± 4.70
Middle	50.5 ± 3.67	50.3 ± 4.79
Bottom	49.9 ± 2.44	49.5 ± 3.98

Table 4. Experimental and simulated uniformity index (λ) values of wheat samples in the plastic container at stationary and moving conditions with the conveyor speed of 14.23 m h^{-1} for 210 and 287 s RF heating, respectively, under an initial temperature of 25 °C and a fixed gap of 120 mm.

Condition	Experimental λ in layers			
	Top	Middle	Bottom	Whole
Stationary	0.2000 ± 0.0115a	0.1588 ± 0.0073a	0.1198 ± 0.0134a	0.1579 ± 0.0022a
Moving	0.1862 ± 0.0030a	0.1394 ± 0.0058b	0.1005 ± 0.0045a	0.1531 ± 0.0026a
	Simulated λ in layers			
Stationary	0.2229	0.1930	0.1649	0.1864
Moving	0.2061	0.1893	0.1624	0.1818

Note: Mean values followed by the same letters within the column are not significantly different ($p > 0.05$).

Table 5. Simulated heating uniformity index of wheat samples in the polypropylene container placing at Position A and Position B under moving conditions with three top electrode lengths at a fixed electrode gap of 12 cm.

	Top electrode length (m)		
	0.50	0.83	1.00
Position A			
Conveyor speed (v_i, m h^{-1})	8.57	14.23	17.14
Estimated total heating time (t_i, s)	336	287	273
Uniformity index (λ_i)	0.1731	0.1818	0.1829
Position B			
Estimated total heating time (t_i, s)	302	266	256
Uniformity index (λ_i)	0.1646	0.1697	0.1712

positions under the top electrode.[49] This non-uniform electric field intensity distribution over the load could be simulated by moving the container with a discrete distance, which was successfully conducted in modeling microwave heating with a turntable.[33,34] To balance accurate temperature predictions and the simulation time, appropriate time steps could be selected to simulate the transient and final temperature distributions in wheat samples on the conveyor belt. This is the next step for our research in developing postharvest RF disinfestations method for industrial applications.

4. Conclusions

A computer model of RF heating for the stationary and moving wheat samples was developed using the finite element-based commercial software, COMSOL. Good agreements were obtained when comparing the simulated and experimental temperatures in three horizontal layers of wheat sample under stationary and moving conditions, and both showed higher

temperatures in the middle and bottom layers compared with those of the top layer. Corners and edges were heated more than central parts in all three layers. The validated model was further used to predict the influences of conveyor movement speeds, three different top electrode lengths, and turning the container by 90° under moving conditions on heating uniformity. Simulated results showed that moving and turning the container by 90° could improve the RF heating uniformity. This simplified and effective simulation approach could be effectively used to understand and analyze the effects of conveyor movement on RF heating uniformity.

Acknowledgments

We thank all members of agricultural product processing laboratory for their helps.

Disclosure statement

No potential conflict of interest was reported by the authors.

References

[1] Gao M, Tang J, Villa-Rojas R, et al. Pasteurization process development for controlling Salmonella in in-shell almonds using radio frequency energy. J. Food Eng. 2011;104:299–306.
[2] Kim S-Y, Sagong H-G, Choi SH, et al. Radio-frequency heating to inactivate Salmonella Typhimurium and Escherichia coli O157:H7 on black and red pepper spice. Int. J. Food Microbiol. 2012;153:171–175.
[3] Jeong SG, Kang DH. Influence of moisture content on inactivation of Escherichia coli O157:H7 and Salmonella enterica serovar Typhimurium in powdered red and black pepper spices by radio-frequency heating. Int. J. Food Microbiol. 2014;176:15–22.
[4] Nelson SO. Insect-control studies with microwaves and other radio frequency energy. Bull. ESA. 1973;19:157–163.
[5] Nelson S, Payne J. RF dielectric heating for pecan weevil control. Trans. ASAE. 1982;31:456–458.
[6] Lagunas-Solar M, Pan Z, Zeng N, et al. Application of radio frequency power for non-chemical disinfestation of rough rice with full retention of quality attributes. Appl. Eng. Agric. 2007;23:647–654.
[7] Shrestha B, Baik O-D. Radio frequency selective heating of stored-grain insects at 27.12 MHz: a feasibility study. Biosyst. Eng. 2013;114:195–204.
[8] Rajhi A. Optimization of the EM heating cycle by using a dual frequency local hyperthermia applicator. J. Electromagn. Waves Appl. 2003;17:447–464.
[9] Mohsin SA, Sheikh NM, Abbas W. MRI induced heating of artificial bone implants. J. Electromagn. Waves Appl. 2009;23:799–808.
[10] Jiao S, Johnson JA, Tang J, et al. Industrial-scale radio frequency treatments for insect control in lentils. J. Stored Prod. Res. 2012;48:143–148.
[11] Zhu H, Huang Z, Wang S. Experimental and simulated top electrode voltage in free-running oscillator radio frequency systems. J. Electromagn. Waves Appl. 2014;28:606–617.
[12] Wang S, Tang J, Cavalieri R, et al. Differential heating of insects in dried nuts and fruits associated with radio frequency and microwave treatments. Trans. ASAE. 2003;46:1175–1184.
[13] Tiwari G, Wang S, Tang J, et al. Computer simulation model development and validation for radio frequency (RF) heating of dry food materials. J. Food Eng. 2011;105:48–55.
[14] Alfaifi B, Tang J, Jiao Y, et al. Radio frequency disinfestation treatments for dried fruit: model development and validation. J. Food Eng. 2014;120:268–276.

[15] Wang S, Yue J, Tang J, et al. Mathematical modelling of heating uniformity for in-shell walnuts subjected to radio frequency treatments with intermittent stirrings. Postharvest Biol. Technol. 2005;35:97–107.
[16] Gao M, Tang J, Wang Y, et al. Almond quality as influenced by radio frequency heat treatments for disinfestation. Postharvest Biol. Technol. 2010;58:225–231.
[17] Pan L, Jiao S, Gautz L, et al. Coffee bean heating uniformity and quality as influenced by radio frequency treatments for postharvest disinfestations. Trans. ASABE. 2012;55:2293–2300.
[18] Koskiniemi CB, Truong V-D, Simunovic J, et al. Improvement of heating uniformity in packaged acidified vegetables pasteurized with a 915 MHz continuous microwave system. J. Food Eng. 2011;105:149–160.
[19] Pedreño-Molina JL, Monzó-Cabrera J, Catalá-Civera JM. Sample movement optimization for uniform heating in microwave heating ovens. Int. J. RF Microwave Comput. Aided Eng. 2007;17:142–152.
[20] Koskiniemi CB, Truong V-D, McFeeters RF, et al. Quality evaluation of packaged acidified vegetables subjected to continuous microwave pasteurization. LWT - Food Sci. Technol. 2013;54:157–164.
[21] Wang S, Tiwari G, Jiao S, et al. Developing postharvest disinfestation treatments for legumes using radio frequency energy. Biosyst. Eng. 2010;105:341–349.
[22] Birla SL, Wang S, Tang J, et al. Improving heating uniformity of fresh fruit in radio frequency treatments for pest control. Postharvest Biol. Technol. 2004;33:205–217.
[23] Wang S, Birla SL, Tang J, et al. Postharvest treatment to control codling moth in fresh apples using water assisted radio frequency heating. Postharvest Biol. Technol. 2006;40:89–96.
[24] Tiwari G, Wang S, Birla SL, et al. Effect of water assisted radio frequency heat treatment on the quality of 'Fuyu' persimmons. Biosyst. Eng. 2008;100:227–234.
[25] Neophytou RI, Metaxas AC. Computer simulation of a radio frequency industrial system. J. Microw. Power Electromagn. Energy. 1996;31:251–259.
[26] Neophytou R, Metaxas A. Combined 3D FE and circuit modeling of radio frequency heating systems. J. Microw. Power Electromagn. Energy. 1998;33:243–262.
[27] Chan TV, Tang J, Younce F. 3-Dimensional numerical modeling of an industrial radio frequency heating system using finite elements. J. Microw. Power Electromagn. Energy. 2004;39:87–105.
[28] Yang J, Zhao Y, Wells JH. Computer simulation of capacitive radio frequency (RF) dielectric heating on vegetable sprout seeds. J. Food Process Eng. 2003;26:239–263.
[29] Marra F, Lyng J, Romano V, et al. Radio-frequency heating of foodstuff: Solution and validation of a mathematical model. J. Food Eng. 2007;79:998–1006.
[30] Wang J, Olsen RG, Tang J, et al. Influence of mashed potato dielectric properties and circulating water electric conductivity on radio frequency heating at 27 MHz. J. Microw. Power Electromagn. Energy. 2008;42:31–46.
[31] Birla SL, Wang S, Tang J. Computer simulation of radio frequency heating of model fruit immersed in water. J. Food Eng. 2008;84:270–280.
[32] Geedipalli SSR, Rakesh V, Datta AK. Modeling the heating uniformity contributed by a rotating turntable in microwave ovens. J. Food Eng. 2007;82:359–368.
[33] Liu S, Fukuoka M, Sakai N. A finite element model for simulating temperature distributions in rotating food during microwave heating. J. Food Eng. 2013;115:49–62.
[34] Pitchai K, Chen J, Birla S, et al. A microwave heat transfer model for a rotating multi-component meal in a domestic oven: development and validation. J. Food Eng. 2014;128:60–71.
[35] Chen H, Tang J, Liu F. Simulation model for moving food packages in microwave heating processes using conformal FDTD method. J. Food Eng. 2008;88:294–305.
[36] Resurreccion FP, Luan D, Tang J, et al. Effect of changes in microwave frequency on heating patterns of foods in a microwave assisted thermal sterilization system. J. Food Eng. 2015;150:99–105.
[37] Metaxas A. Foundations of Electroheat. A Unified Approach. Fuel and Energy Abstracts. Elsevier Science; 1996.
[38] Choi C, Konrad A. Finite element modeling of the RF heating process. IEEE Trans. Magn. 1991;27:4227–4230.

[39] Jiao Y, Tang J, Wang S, et al. Influence of dielectric properties on the heating rate in free-running oscillator radio frequency systems. J. Food Eng. 2014;120:197–203.
[40] Huang Z, Zhu H, Yan R, et al. Simulation and prediction of radio frequency heating in dry soybeans. Biosyst. Eng. 2015;129:34–47.
[41] Wang S, Tang J, Cavalieri R. Modeling fruit internal heating rates for hot air and hot water treatments. Postharvest Biol. Technol. 2001;22:257–270.
[42] Barber H. Electroheat. 1st ed. London: Granada Publishing; 1983.
[43] Marshall MG, Metaxas AC. Modeling of the radio frequency electric field strength developed during the RF assisted heat pump drying of particulates. J. Microw. Power Electromagn. Energy. 1998;33:167–177.
[44] Wang S, Monzon M, Johnson JA, et al. Industrial-scale radio frequency treatments for insect control in walnuts. Postharvest Biol. Technol. 2007;45:240–246.
[45] COMSOL. Material library V4.3a, Burlington: COMSOL Multiphysics; 2012.
[46] von Hippel AR. Dielectric materials and applications. Boston, MA: Arctech House; 1995.
[47] Li Y, Zhang L, Cao Y, et al. Determination of thermal conductivity of wheat. Henan Univ. Technol.: Nat. Sci. 2010;31:67–70.
[48] Wang S, Monzon M, Johnson JA, et al. Industrial-scale radio frequency treatments for insect control in walnuts. Postharvest Biol. Technol. 2007;45:240–246.
[49] Wang Y, Zhang L, Gao M, et al. Evaluating radio frequency heating uniformity using polyurethane foams. J. Food Eng. 2014;136:28–33.